2015 IEEE International Conference on
Automation Science and Engineering (CASE)
Aug 24-28, 2015. Gothenburg, Sweden

Pose Statistics for Eccentric Parts

Fatemeh Panahi[1], Aviv Adler[2] and A. Frank van der Stappen[1]

***Abstract*— In many contexts, it is very useful to have an estimate of the final orientation, or *pose*, of an object which is dropped onto a flat surface. In this paper, we consider the final orientation of an object which starts with a random orientation, and show how the shape of the object relates to the distribution of its final orientation. We define a notion of *geometric eccentricity* for d-dimensional objects, which takes into account both its shape and its center-of-mass. We show that under quasi-static conditions, the pose into which eccentric objects settle will be with high probability in a cluster of poses which are very close together. Furthermore, the probability of ending up in this range of poses increases, and the size of the range decreases, as the object gets more eccentric.**

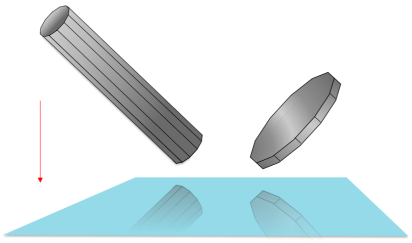

Fig. 1. Examples of eccentric objects

I. Introduction

For many automated manufacturing tasks, it is important to predict the behavior of the parts being manufactured as they are manipulated. Parts often have to be oriented with part feeders before they are put through assembly lines [1]; the shape of the part is usually known, but its starting orientation or location is not. The basic objective of part feeders is to minimize the uncertainty on the orientation of the part before the next stage of the manufacturing process. This is often achieved by applying a sequence of actions on a stream of identical parts which produce a fixed final orientation regardless of initial orientation. There are various part feeding systems which have been thoroughly studied. Orienting a part using sensorless feeding designs based on a finite set of actions has been studied [2], [3]; for example, it has been shown that there always exists a way to orient a polygonal part by pushing or squeezing using a frictionless parallel jaw gripper [4], [5]. There are also approaches that are based on constrained forms of pushing. A system consisting of a conveyor belt with fences mounted to its sides is considered in [6]. Parts are oriented by sliding along the fences while traveling on the belt. Erdmann et al. considered a three dimensional part lying on a planar table with infinite friction [7]. The table is then given a sequence of tilts which reduces the uncertainty of the orientation of the part.

A common assumption in most of the aforementioned studies is that the parts are already resting in contact with the worksurface. However, it is also useful to consider how parts will arrive on the supporting surface when their initial pose is unknown. When a part arrives on the surface, it settles into an orientation such that it does not topple over under the influence of gravity; this is called a *stable pose*. Evaluating the stable poses of an object allows estimation of the likelihood of what orientation it will arrive in, which can result in faster and more effective design of part feeders as well as many other automated tasks. There are a number of works estimating the probability distribution over a part's stable poses where its initial orientation with the worksurface is uniformly at random and the part falls on a flat worksurface in presence of gravity [8]–[12]. Wiegley et al. [13] proposed an $O(n^2)$ time algorithm for estimating the distribution of stable poses of an n-sided polyhedron under quasi-static conditions (i.e. without dynamics). Mirtich et al. [14] developed this algorithm further by considering a simple model of dynamic stability. They discussed the results from full dynamic Monte Carlo simulation and they compared the algorithms to real data. The notion of a *capture region*, the region in configuration space in which any initial configuration will converge to a given final configuration, was introduced in [15]. Moll and Erdmann [16], [17] studied the pose distribution for an object being dropped on a sloped surface or into a curved bowl. In particular, they showed that by controlling the height and initial velocity of the part, and the shape of the bowl, it was possible to greatly reduce uncertainty on the final orientation of the part. Recently, Várkonyi [18] created a simulated dataset and evaluated the estimators proposed in the literature by comparing their predictions to simulation results; he also proposed new estimation algorithms.

For some parts, it is possible to predict that the pose which they settle into will (with high probability) be in a cluster of poses which are very close together. Considering these poses as the most probable initial orientations of the part for feeding allows faster design for part feeding tasks. Observing the usefulness of bias in pose distribution for part feeding, we consider a variant of the notion of *geometric eccentricity* for objects and show that there is a high probability for an

[1] Department of Information and Computing Sciences, Utrecht University, Utrecht, The Netherlands. f.panahi@uu.nl, a.f.vanderstappen@uu.n

[2] Department of Electrical Engineering and Computer Science, Massachusetts Institute of Technology, Cambridge, MA, USA. adlera@mit.edu

F. Panahi is supported by the Netherlands Organization for Scientific Research (NWO)

eccentric object being dropped on a flat surface to come to the rest in a small range of stable orientations. Broadly, eccentricity is the degree to which a part deviates from being uniformly wide; generally, eccentric objects are long and thin or wide and flat.

Fig. 1 illustrates two 3D objects in presence of gravity on top of a flat surface which have the center of mass at their centroids. The pencil-shape object is longer in one dimension, and the coin-shape object is longer in two dimensions. It is easy to see that the pencil-shaped object is more likely to rest at one of its long sides and the coin-shaped object will rest at one of its two larger sides. Considering the set of final orientations where these objects end up with high probability, they lie on a single plane (for the pencil-shaped object) or on a single line (for the coin-shaped object). This example reveals the intuition behind our definition for geometric eccentricity. Using this definition in 3D, we show that for objects similar to pencil, there is a plane for which the final orientation is, with high probability, going to end up near; for objects similar to coin there is a line which the final orientation is going to end up near as well.

A definition for the geometric eccentricity of a planar part based on the aspect ratio of a distinguished bounding box was already shown to lead to a remarkable upper bound on the number push or squeeze actions required to orient a part with a parallel jaw gripper [19]. Here we propose a much more general notion of geometry eccentricity that not only applies in any dimension but also distinguishes between different types of object eccentricity. Using the presented definition of eccentricity, we study the problem of pose statistics for eccentric objects being dropped on a flat horizontal surface where the only force acting on the object is gravity.

Fatness is a shape-related notion that has led to improved bounds or better solutions to many problems in the field of computational geometry. There are many different definitions for fatness. (A fairly recent survey of the results can be found in [20]). Intuitively, a fat object is an object in two or more dimensions, whose lengths in the different dimensions are similar. We note that eccentricity can be regarded as the opposite (or lack) of fatness.

II. Preliminaries

We assume that the object's center of mass is given and assume without loss of generality that it lies at the origin. Since the surface onto which the object is dropped is flat, the computations can be equivalently performed on the convex hull of the object. Therefore, in this paper we assume without loss of generality that the object is convex.

A. Basic Notation and Definitions

We first establish some basic notation and definitions relating to the geometric properties of the convex object. We use S^{d-1} to refer to the set of *directions* in d-dimensional space, i.e. $S^{d-1} := \{u \in \mathbb{R}^d | \|u\| = 1\}$.

We now consider a convex (closed) object $P \subseteq \mathbb{R}^d$ with center-of-mass at the origin O (where $O \in P$). We model its orientation at any time as a vector $u \in S^{d-1}$; given the object in some orientation above a flat horizontal surface, this vector is the direction of gravity, i.e. it is the unit vector which is perpendicular to the surface. We refer to the surface as the *floor*.

We can then define the *radius function* of P as the distance from the center-of-mass to the floor of an object in a given orientation u (which is touching the floor).

Definition 1 (Radius Function): Given a convex bounded set $P \subset \mathbb{R}^d$ containing the origin, we define the *radius function*, $r_P : S^{d-1} \to \mathbb{R}$ as

$$r_P(u) := \max_{x \in P}(x \cdot u)$$

Finally, we define the *contact set* where an object in a given orientation u intersects the floor.

$$C_P(u) := \{x \in P | x \cdot u = r_P(u)\}.$$

We also note that $C_P(u)$ is convex and closed (as the intersection of two closed, convex sets, P and the plane representing the floor); thus there must be a *unique* point of $C_P(u)$ which is closest to the center-of-mass. This allows the following definition, which we refer to as the *pivot point* because (as we will see) under the quasistatic motion model the object pivots about this point if in orientation u.

Definition 2 (Pivot Point): Given object P containing O, and orientation u, $c_P(u) := \operatorname{argmin}_{x \in C_P(u)} \|x\|$.

Definition 3 (Probability of a Set of Poses): Let Θ be a set of orientations in S^{d-1}. We define ρ as the probability that a uniformly randomly chosen unit vector is in Θ. Mathematically, $\rho(\Theta) = volume(\Theta)/volume(S^{d-1})$, where $volume$ refers to the $(d-1)$-dimensional volume. (This resembles a generalized notion of *solid angle* in geometry.)

B. Quasistatic Model

We assume that the only force acting on the object is gravity and for simplicity we do not consider dynamics. When an object is dropped onto a flat horizontal surface, it moves downward until it contacts the surface. If the center-of-mass is not directly over a point where the object contacts the surface then it will rotate so the center-of-mass descends as quickly as possible. The same quasistatic model has been considered in some previuse work such as [13]. We refer to such an orientation as an *unstable* orientation. If the center-of-mass is directly over a contact point then we have an *equilibrium* orientation. These equilibria correspond to the local mimima and maxima of the radius function. If no (local) rotation of the part will lead to a descent of the center-of-mass then the equilibrium is *stable*.

C. Geometric Eccentricity

The definition of eccentricity that we propose applies to d-dimensional objects and captures the property that an object is a considerable factor, say k, bigger in b of its dimensions than in any of the remaining $d-b$ dimensions. It generalizes an earlier strictly 2D notion based on the aspect ratio of a bounding box [19] and allows us to distinguish between 3D objects similar to the pencil and similar to the coin in Fig. 1.

Definition 4 ((b)-Eccentricity): Let $P \subset \mathbb{R}^d$ be a bounded convex set with its center of mass at the origin O. For any

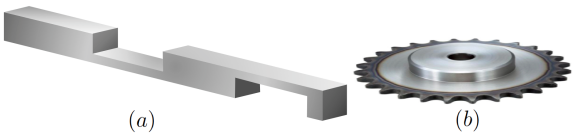

Fig. 2. Examples of (a) an 8-(1)-eccentric object and (b) an 8-(2)-eccentric object.

$1 \leq b < d$, the set P is said to be k-(b)-*eccentric* for some $k \geq 1$ if there exists a scaled and rotated copy of P such that

- the projection of P onto the subspace spanned by b of its dimensions contains the b-dimensional sphere of radius k centered at O, and
- the projection of P onto the subspace spanned by the remaining $d-b$ dimensions is contained in the $(d-b)$-dimensional sphere of unit radius centered at O.

For brevity we will sometimes simply refer to an object that is (b)-eccentric for some b as an eccentric object.

Although the definition of eccentricity applies to parts in any dimension, our focus in this paper is on three-dimensional (and to a lesser extent on two-dimensional) objects. Three-dimensional eccentric objects can be (1)-eccentric or (2)-eccentric: Fig. 2 (a) and (b) show two 3D objects whose convex hulls are 8-(1)-eccentric and 8-(2)-eccentric respectively. We observe that 3D objects can be k-(1)-eccentric and k'-(2)-eccentric at the same time, for not necessarily equal k and k'. Two-dimensional objects can only be (1)-eccentric. As a result, we will often refer to a k-(1)-eccentric 2D object as a k-eccentric object. We note that a two-dimensional object that is k-eccentric according to the definition in [19] is $k+1$-eccentric according to our definition.

III. Pose and Probabilities

In this section, we establish lower bounds on the probabilities of a 3D object ending up in a bounded range of final poses when the initial pose is chosen uniformly at random. We will first introduce three types of orientations, then prove properties for each of these three types, and then use these properties to deduce bounds that depend on the eccentricity parameter k.

In the remainder of the paper we assume without loss of generality that

- a 3D k-(1)-eccentric object is oriented and scaled such that its projection onto the x-axis contains the interval $[-k,k]$ and its projection onto the (y,z)-plane is contained in a unit disc centered at O, and
- a 3D k-(2)-eccentric object is oriented and scaled such that its projection onto the (x,z)-plane contains a disc of radius k centered at O and its projection onto the y-axis is contained in the interval $[-1,1]$, and
- a 2D k-eccentric object is oriented and scaled such that its projection onto the x-axis contains the interval $[-k,k]$ and its projection onto the y-axis is contained in the interval $[-1,1]$.

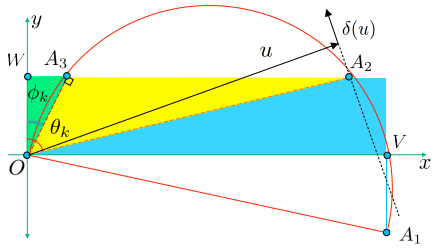

Fig. 3. Types of orientations

A. Types of Poses

We focus on 3D objects with eccentricity $k > 2\sqrt{2}$. It is not surprising that we do not get results for parts with low eccentricity as such parts can have stable poses scattered all over the sphere of directions.

We first decompose S^1.

Definition 5 (Orientation Types in S^1): For a given $k > 2\sqrt{2}$, let D be the disc in $\mathbb{R}^2$ with diagonal OA_1, where $A_1 = (k,-1)$ (see Fig. 3). The boundary of the disc D has two intersection point with $y = 1$ since $k > 2\sqrt{2}$. Let A_2 and A_3 be the intersection points with the larger and smaller x-coordinates respectively. It follows that $A_2 = ((k+\sqrt{k^2-8})/2, 1)$ and $A_3 = ((k-\sqrt{k^2-8})/2, 1)$. In addition, let $W = (0,1)$ and V be the intersection of D with $y = 0$; note that $V = (k,0)$. The orientations in $[0, \pi/2]$, or, in other words, the directions between OV and OW, are divided into three sectors by OA_2 and OA_3. Consider the orientations in S^1 (which correspond to rays emanating from the origin):

- The directions between OV and OA_2 and their images after mirroring in x-axis, y-axis, and O are *type-1* orientations.
- The directions between OA_2 and OA_3 and their images after mirroring in x-axis, y-axis, and O are *type-2* orientations.
- The directions between OA_3 and OW and their images after mirroring in x-axis, y-axis, and O are *type-3* orientations.

The type-1, type-2, and type-3 orientations will be displayed as *blue*, *yellow*, and *green* (respectively) in our figures.

The decomposition of S^1 induces separate decompositions of S^2 into orientation types associated with (1)-eccentric and (2)-eccentric objects.

Definition 6 (Orientation Types in S^2): Let $k > 2\sqrt{2}$.

- The orientation types in S^2 associated with (1)-eccentric parts are obtained by rotating the decomposition of S^1 about the x-axis.
- The orientation types in S^2 associated with (2)-eccentric parts are obtained by rotating the decomposition of S^1 about the y-axis.

Figure 4 shows both decompositions of S^2.

The following property connects the eccentricity of 3D objects to the eccentricity of their 2D projections.

Property 1: Let P be a 3D object:

- The projection of P onto any plane containing the x-axis is a 2D k-eccentric object if P is k-(1)-eccentric.

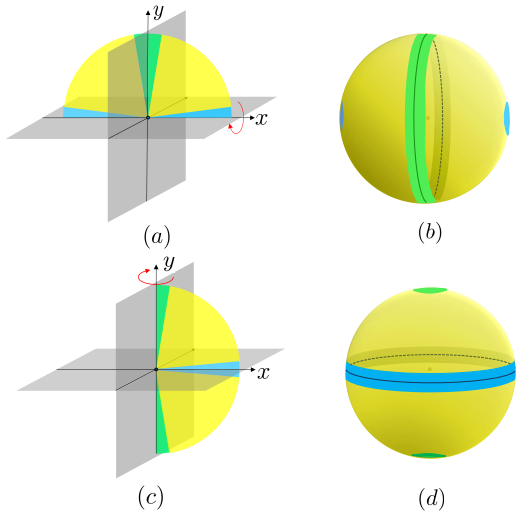

Fig. 4. **(a)**The three types of orientations in a xy^+ plane for a k-eccentric 2D object. **(b)** Representation of *all* orientations for a k-(1)-eccentric 3D object. **(c)** The three types of orientations in a x^+y plane for a k-eccentric 2D object. **(d)** Representation of *all* orientations for a k-(2)-eccentric 3D object. Any object that is initially in a type-2 or type-3 orientation will end up at a type-3 orientation.

- The projection of P onto any plane containing the y-axis is a 2D k-eccentric object if P is k-(2)-eccentric.

B. Properties of Poses

In this subsection we will establish that a 3D object that is initially in a type-2 or type-3 pose must end up in a type-3 pose.

Lemma 2: Type-2 poses are unstable.

Proof: Let $P \subset \mathbb{R}^3$ be k-(1)-eccentric or k-(2)-eccentric and assume for contradiction that it has a type-2 stable pose θ in S^2. Let Z be the tangent plane to P perpendicular to θ. Since θ is stable, the point of contact between Z and P must lie on θ. Now we rotate P, along with θ and Z, around the x-axis if P is k-(1)-eccentric and around the y-axis if P is k-(2)-eccentric to get (without changing the situation) θ to lie in the (x, y)-plane. Let Q be the projection of P onto the (x, y)-plane. By Property 1, Q is a k-eccentric planar object. Note that within the (x, y)-plane the direction θ now corresponds to a type-2 pose in S^1. If θ cannot be stable for Q then it cannot be stable for P since the supporting line of Q perpendicular to θ equals the intersection of Z with the (x, y)-plane. Therefore, it is enough to show that θ cannot correspond to a stable pose for Q. Note that a tangent line of Q perpendicular to any stable orientation, has a contact point at which the normal vector passes through the center of mass. In addition, since Q is a k-eccentric planar object, it has a point on $x = k$ in the interval $[-1, 1]$ for y. According to the definition of planar type-2 orientations, θ lies between OA_2 and OA_3. For any stable orientation, in this range (between OA_2 and OA_3) the perpendicular tangent line does not intersect the line $x = k$ in the interval $[-1, 1]$ for y, which is in contradiction with the assumption that Q is convex, thus proving the lemma. ■

Lemma 3: A k-(1)-eccentric or k-(2)-eccentric object $P \subset \mathbb{R}^3$ that is initially at a type-2 or type-3 pose ends up at a type-3 pose.

Proof: We define the *long axes* as the x-axis in the k-(1)-eccentric case and the (x, z)-plane in the k-(2)-eccentric case. For any orientation u, we define $\alpha(u)$ to be the minimum angle between u and any orientation v contained in the long axes. We note that trivially, $\alpha(u)$ is smaller for any type-1 orientation than for any type-2 or type-3 orientation (i.e. if u_1 is type-1 and u_2 is not type-1, then $\alpha(u_1) < \alpha(u_2)$).

What we now show is that as the part rotates, $\alpha(u)$ cannot decrease; this means that if it starts in a type-2 or type-3 orientation, it cannot enter the region of type-1 orientations since this would mean decreasing $\alpha(u)$. Thus, it must settle on a non-type-1 stable pose; however, since there are no type-2 stable poses (by Lemma 2), this means that the final pose must be type-3.

We base our proof on the notation given in Fig. 3. Suppose that the current orientation u is type-2. Without loss of generality, we can assume that u lies on the (x, y)-plane. Note that for a k-(1)-eccentric object it can be rotated around x-axes and for a k-(2)-eccentric object the object can be rotated around y-axes. Then, u corresponds to the yellow range in Fig. 3. We note that in this case, the pivot point $c_P(u)$ (see Definition 2) must be a type-1 orientation (not necessarily in the (x, y)-plane) and therefore closer (in angle) to V than u is to V; this is because the $c_P(u)$ must be between $y = -1$ and $y = 1$. Thus, if it weren't closer to V then $c_P(u) \cdot u$ is less than the distance of any point on the far right side of $x = k$ projected onto the line containing u; but due to the object eccentricity there must be some point v there, and in that case $v \cdot u > c_P(u) \cdot u$. But this contradicts the definition of $c_P(u)$, thus proving that

$$\angle c_P(u)OV < \angle uOV.$$

We now consider the direction which the object is rotating in when it is in orientation u; this can be expressed by a unit vector $\delta(u)$ which is perpendicular to u, i.e. $u \cdot \delta(u) = 0$. Note that $\delta(u)$ is in the plane passing through u, $c_P(u)$ and the origin. Suppose we are rotating in such a way as to get closer to $c_P(u)$, i.e. if $\delta(u) \cdot (c_P(u) - u) > 0$; this will cause the radius to increase (i.e. the center of mass to rise). This is impossible, so $\delta(u) \cdot (c_P(u) - u) \leq 0$. But since $c_P(u)$ is closer in angle to V than u is,

$$\delta(u) \cdot (c_P(u) - u) \leq 0 \implies \delta(u) \cdot (V - u) \leq 0.$$

Thus, the angle between the current pose u and V (the long axis in Fig. 3) is never increasing as long as u is type-2. Thus, starting from a type-2 or type-3 orientation cannot lead to a type-1 final orientation, completing the proof. ■

Lemma 2 shows that type-2 orientations are unstable. The remaining orientations are *potentially stable* orientations. The stable orientations in type-1 have radii larger than $|OA_2|$ the stable orientations in type-3 have radii smaller than $|OA_3|$.

Lemmas 2 and 3 and the trivial fact that a part cannot settle in an unstable orientation reveal that objects that are

initially in a type-2 or type-3 orientation will end up in type-3 orientation and objects that are initially in a type-1 orientation will end up in a type-1 or type-3 orientation. In other words, objects in yellow or green poses in Fig. 4 will end up in a green final pose and objects in a blue pose will end up in blue or green final pose. The following theorem summarizes the former (non-trivial) part of this conclusion in terms of probabilities.

Theorem 4: Let $P \subset \mathbb{R}^3$ be a k-(1)-eccentric or k-(2)-eccentric object ($k > 2\sqrt{2}$) in a uniformly random initial orientation. The probability of P ending up at type-3 orientations is at least $\rho(\Theta)$ where Θ is the union of the set of type-2 and type-3 orientations.

We observe that the final orientations lie in the proximity of a plane, the (y,z)-plane if P is k-(1)-eccentric and the (x,z)-plane if P is k-(2)-eccentric, and the proximity of a line, the x-axis if P is k-(1)-eccentric the y-axis if P is k-(2)-eccentric. Theorem 4 gives a lower bound on the probability for (or bias towards) the plane if P is k-(1)-eccentric and the line if P is k-(2)-eccentric. In the next subsection we will see that lower bounds as well as the sizes of the proximities depends on k.

C. Computing the Probabilities

In this subsection we will obtain an upper bound on the size of the set of type-3 orientations in which the part will settle with a probability that equals at least the fraction of S^2 covered by type-2 and type-3 orientations. We will also derive an upper bound on the size of the set of type-1 and type-3 orientations in which the object is guaranteed to settle. Although similar bounds for 2D objects are easy to obtain we focus solely on 3D objects. We define $\Phi_k^{(i)}$, $\Theta_k^{(i)}$, and $\Psi_k^{(i)}$ (with $i = 1, 2$) to be the sets of all type-3, union of type-2 *and* type-3, and type-1 orientations in S^2 for a k-(i)-eccentric object, respectively.

We recall Definition 5 and let $\theta_k = \measuredangle A_2OW$ and $\phi_k = \measuredangle A_3OW$. Note that θ_k and ϕ_k are the angles in S^1 relative to the y-axis that mark the boundaries between type-1 and type-2 orientations and between type-2 and type-3 orientations respectively. By Definition 6 these angles also determine the boundaries between the corresponding types of orientations in S^2. (See Fig. 3.) From Definition 5 it follows that

$$\theta_k = \arctan\left(\frac{k + \sqrt{k^2 - 8}}{2}\right) \tag{1}$$

$$\phi_k = \arctan\left(\frac{k - \sqrt{k^2 - 8}}{2}\right) \tag{2}$$

Using the well-known fact that the surface area of a segment or cap of height h of the unit sphere equals $2\pi h$ and observing that $\Phi_k^{(i)}$, $\Theta_k^{(i)}$, and $\Psi_k^{(i)}$ can all be regarded as unions of two segments or caps we obtain

$$\begin{aligned}
\rho(\Theta_k^{(1)}) &= \frac{2}{4\pi}(2\pi \sin\theta_k) = \sin\theta_k \\
\rho(\Phi_k^{(1)}) &= \frac{2}{4\pi}(2\pi \sin\phi_k) = \sin\phi_k \\
\rho(\Psi_k^{(1)}) &= \frac{2}{4\pi}(2\pi(1 - \sin\theta_k)) = 1 - \sin\theta_k,
\end{aligned} \tag{3}$$

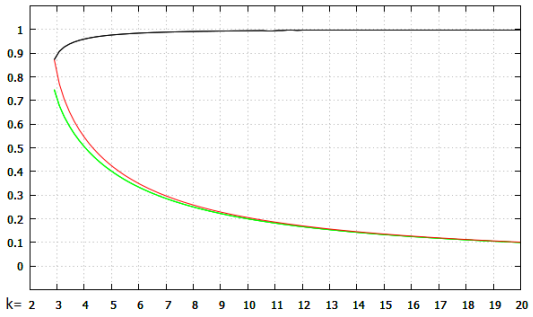

Fig. 5. The graph of $\rho(\Theta_k^{(1)})$, $\rho(\Phi_k^{(1)})$, and $\rho(\Phi_k^{(1)} \cup \Psi_k^{(1)})$ illustrated in black, green, and red, respectively for a k-(1)-eccentric object.

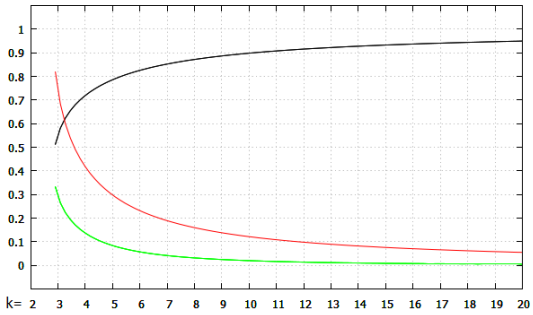

Fig. 6. The graph of $\rho(\Theta_k^{(2)})$ and $\rho(\Phi_k^{(2)})$, and $\rho(\Phi_k^{(2)} \cup \Psi_k^{(2)})$ illustrated in black, green, and red, respectively for a k-(2)-eccentric object.

and we also have

$$\begin{aligned}
\rho(\Theta_k^{(2)}) &= \frac{2}{4\pi}(2\pi(1 - \cos\theta_k)) = 1 - \cos\theta_k \\
\rho(\Phi_k^{(2)}) &= \frac{2}{4\pi}(2\pi(1 - \cos\phi_k)) = 1 - \cos\phi_k \\
\rho(\Psi_k^{(2)}) &= \frac{2}{4\pi}(2\pi \cos\theta_k)) = \cos\theta_k.
\end{aligned} \tag{4}$$

We can now use these equations, Theorem 4, and the observation that no part can settle in a type-2 pose to formulate our main result.

Theorem 5: Let $P \subset \mathbb{R}^3$ be a k-(1)-eccentric or k-(2)-eccentric object ($k > 2\sqrt{2}$) in a uniformly random initial orientation, and let $\theta_k = \arctan\left((k + \sqrt{k^2 - 8})/2\right)$ and $\phi_k = \arctan\left((k - \sqrt{k^2 - 8})/2\right)$. If P is k-(1)-eccentric then it settles

- with probability at least $\sin\theta_k$ in a spherical segment of orientations symmetrically surrounding a plane that covers a fraction $\sin\phi_k$ of S^2,
- and in one of two antipodal spherical caps of orientations surrounding a line that jointly cover a fraction $1 - \sin\theta_k$ of S^2 otherwise.

If P is k-(2)-eccentric then it settles

- with probability at least $1 - \cos\theta_k$ in one of two antipodal spherical caps of orientations surrounding a line that jointly cover a fraction $1 - \cos\phi_k$ of S^2
- and in one spherical segment of orientations symmetrically surrounding a plane that covers a fraction $\cos\theta_k$ of S^2 otherwise.

The theorem shows that the sizes of the caps and segment in which P is guaranteed to settle shrink if k increases, so the uncertainty about the final pose decreases. Moreover, it shows that the bias towards the segment (or plane) if P is k-(1)-eccentric and towards the caps (or line) if P is k-(2)-eccentric increases if k increases (at the cost of the caps and segment respectively). Another way of stating the theorem is as follows; for k-(1)-eccentric objects, with probability $sin\theta_k$, the final orientation has at most ϕ_k distance from a plane and for k-(2)-eccentric objects, with probability $1 - cos\theta_k$, the final orientation has at most $\pi/2 - \theta_k$ distance from a line. Fig. 5 and 6 provide insight into how the sizes of the sets and the probabilities vary as a function of k.

Fig. 5 shows that a 8-(1)-eccentric part always settles in a region containing less than 26% of the orientations and with a probability that is close to 99% in a region containing less than 25% of the orientations. Fig. 6 shows that a 8-(2)-eccentric part always settles in a region of less than 15% of the orientations and with a probability that is close to 89% in less then 4% of the orientations. It can be observed that for larger k, there is a smaller range of poses that the object always can settle in and there is a higher probability for the object to settle in again smaller range of poses.

IV. Conclusions

In this paper, we studied the pose statistics problem for a family of 3D objects with initial pose, uniformly at random. We assumed that the object falls onto a flat surface in presence of gravity under the quasi-statics conditions. We proposed a novel type of geometric eccentricity for d-dimensional objects for which the final distribution of 3D objects have a substantial bias towards a small range of poses when they come to rest. This result can be applied to part feeding tasks to obtain a faster design for reducing the object pose uncertainty.

According to our proposed notion of eccentricity, for a given k, we have two types of eccentricity in 3D: k-(1)-eccentric objects are k times bigger in one dimension than the other two dimensions while k-(2)-eccentric objects are k times bigger in two dimensions than the other dimension. We showed that for both types of eccentric objects there is a small cluster of poses at which the object always ends up. We showed that there is a high probability of ending up at a pose which is close to a specific plane for k-(1)-eccentric objects, and close to a specific line for k-(2)-eccentric objects. In addition, we showed that for larger k, there is smaller range of poses (which are close together) at which the k-(1)-eccentric and k-(2)-eccentric objects end up with higher probability.

Our results are based on the quasi-static assumption. The work by Goldberg et al. [**?**] and Várkonyi [18] suggests that our results are therefore conservative because more realistic part behavior models tend to lead to even larger biases towards even smaller ranges of pases. To rigorously show this, it is interesting to explore a model incorporating the dynamics of collisions and friction.

Our analysis of pose statistics for eccentric parts departs from the assumption that the object at hand is known to be k-(1)-eccentric or k-(2)-eccentric. It is therefore natural to consider how k can be computed for a given object P. In particular, to obtain the strongest possible bounds on the bias towards certain poses it is desirable to find the largest k for which P is k-(1)-eccentric or k-(2)-eccentric.

References

[1] G. Boothroyd, C. Poli, and L. E. Murch, Automatic Assembly. New York: Basel, Marcel Dekker, Inc., 1982.

[2] T. Lozano-Perez, M. T. Mason, R. H. Taylor, Automatic synthesis of fine-motion strategies for robots. International Journal of Robotics Research 3(1), pp.3-24, 1984.

[3] M. A. Erdmann and M.T. Mason, An exploration of sensorless manipulation, IEEE Journal of Robotics and Automation 4, pp. 369-379, 1988.

[4] K. Goldberg, Orienting polygonal parts without sensors, Algorithmica 10, pp. 201-225, 1993.

[5] Y. -B. Chen and D. J. Ierardi, The complexity of oblivious plans for orienting and distinguishing polygonal parts, Algorithmica 14, pp. 367-397, 1995.

[6] J. A. Wiegley, K. Goldberg, M. Peshkin, M. Brokowski, A complete algorithm for designing passive fences to orient parts. Assembly Automation, 17(2), pp. 129-136, 1997.

[7] M. Erdmann and M. T. Mason, G. Vaněček, Mechanical parts orienting: The case of a polyhedron on a table. Algorithmica, 10(2), pp. 226-247, 1993.

[8] B. K. A. Ngoi, L. E. N. Lim, and S. S. G. Lee, Analyzing the Probabilities of Natural Resting for a Component With a Virtual Resting Face. Manufacturing Science and Engineering, 120: pp. 468-471, 1998.

[9] B. Mirtich, Y. Zhuang, K. Y. Goldberg, J. Craig, R. Zanutta, B. Carlisle and J. F. Canny, Estimating pose statistics for robotic part feeders. Proc. of the IEEE International Conference on Robotics and Automation, pp.1140-1146, 1996.

[10] G. Boothroyd and C. Ho, Natural resting aspects of parts for automatic handling. Journal of Engineering for Industry, vol. 99, pp. 314-317, 1977.

[11] P. S. K. Chua and M. L. Tay, Modelling the natural resting aspect of small regular shaped parts. *Manufacturing Science and Engineering*, 120: pp. 540-546, 1998.

[12] S. S. G. Lee, B. K. A. Ngoi, L. E. N. Lim, and S. W. Lye, Determining the probabilities of natural resting aspects of parts from their geometries. Assembly Automation, 17: pp. 137-142, 1997.

[13] J. Wiegley, A. Rao, and K. Goldberg, Computing a statistical distribution of stable poses for a polyhedron, Proc. of Allerton Conference Communications, Control and Computing, 1992.

[14] K. Goldberg, B. Birtich, Y. Zhuang, J. Craig, B. Carlisle, and J. Canny. Part Pose Statistics: Estimators and Experiments. IEEE Transactions on Robotics and Automation. 15(5), pp. 849-857, 1999.

[15] D. J. Kriegman, Let them fall where they may: Capture regions of curved objects and polyhedra, International Journal of Robotics Research, 16(4):448-472, 1997.

[16] M. Moll and M. A. Erdmann, Manipulation of Pose Distributions, Robotics Research, 21(3), pp. 277-292, 2002.

[17] M. Moll and M. A. Erdmann, Uncertainty Reduction Using Dynamics, Proc. IEEE International Conference on Robotics and Automation, pp. 3673-3680, 2000.

[18] P. L. Várkonyi, Estimating part pose statistics with application to industrial parts feeding and shape design: new metrics, algorithms, simulation experiments and datasets. IEEE Transactions on Robotics and Automation, 11, pp. 658-667, 2014.

[19] A. F. van der Stappen, K. Goldberg and M. H. Overmars, Geometric eccentricity and the complexity of manipulation plans, Algorithmica 26(3/4), pp. 494-514, 2000.

[20] C. M. Gray, Algorithms for Fat Objects: Decompositions and Applications. Ph. D. Dissertation, Technische Universiteit Eindhoven, Netherlands, 2008.

[21] N. B. Zumel, A Non-prehensile Method for Reliable Parts Orienting. PhD thesis, Robotics Institute, Carnegie Mellon University, Pittsburgh, PA, 1997.